DEGRADATION OF SOLAR CELL ELECTRIC PERFORMANCE DUE TO ARCING IN LEO PLASMA ENVIRONMENT

Teppei Okumura, Satoshi Hosoda, Jeongho Kim, Mengu Cho
Department of Electrical Engineering, Kyushu Institute of Technology
1-1Sensui Tobata-ku Kitakyushu 804-8550, Japan
Phone & Fax: +81-93-884-3229
E-mail: c346406t@tobata.isc.kyutech.ac.jp

Hideshi Kagawa
JAXA (Japan Aerospace Exploration Agency)

Abstract

When we operate solar array at high voltage (>100V) in LEO environment, arcing occurs on the solar array surface. The solar cell can suffer degradation of electric performance due to only one arc with some probability. We performed degradation test of solar array coupons against arcing under simulated LEO environment in order to identify the threshold of arc energy to cause the solar cell degradation. The solar array coupons are made of silicon solar cells. The LCR circuit was attached to a solar array coupon through a vacuum chamber. In order to change trigger arc energy, we changed the value of capacitance of LCR circuit. The electric performance was measured inside the chamber without opening the chamber. The threshold of arc energy was identified. The arcing which has enough energy to cause the solar cell degradation may occur on solar array of 100V satellite in Low Earth Orbit environment.

Introduction

Recent spacecrafts have larger structures and longer life times years after year. These spacecrafts need a large amount of electric power generation. The International Space Station (ISS) can generate 65kW electric power. The higher bus voltage is necessary for the large spacecraft to minimize transmission loss and reduce the power cable mass. A bus voltage over 100V has been employed for 10kW-satellites, and the power generation voltage of solar array has become over 100V. In the case of ISS, the generation voltage is 160V, and the bus voltage is 120V. In near future, human being will construct more large spacecrafts, such as a space hotel and a space factory. These spacecrafts need larger electric power (>1MW). Generally, the bus voltage is proportional to the square root of electric power. The 1MW-class spacecrafts will need the generation voltage of 400V.

The negative end of solar array is grounded to the structural body in many spacecrafts. Under the Low Earth Orbit (LEO) environment, the space plasma, whose density is of the order of 10^{10}~10^{12}m^{-3}, can charge the spacecrafts at a negative potential with respect to the plasma, because of electron's higher velocity than ions. While the positive end of the solar array has roughly the same potential as the ambient plasma, the spacecraft body and the negative end of the solar array has a negative potential almost equal to the power generation voltage. When the solar array generates the electric power at 400V, most parts of the spacecraft and the solar array have negative potentials with respect to the plasma, especially the negative end of the solar array is -400V.

Arcing is observed on the spacecraft and the solar array, when the spacecraft has the negative potential of from 100V to 200V with respect to the ambient plasma [1][2]. The arcing causes considerable problems, such as power reduction due to solar cell degradation [3][4], electromagnetic interference and destruction of solar array circuit [5]. Seriousness of these problems depends on the arc frequency and energy of each arc. This paper discusses the study of solar cell degradation due to primary arcs.

The cross sectional view of solar array is shown in Fig.1. When solar array has a negative potential relative to the ambient plasma, the solar array attracts ions from ambient plasma. Electric field is generated inside the coverglass, and enhanced near the triple junction, which is the boundary of conductor, dielectric and plasma. Field enhancement at the triple junction induces an arc. The arc plasma expands on the solar array and neutralizes the charged coverglass. Energy of arc is supplied by the charged coverglass. The value of arc energy depends on the generation voltage and the expansion area of the arc plasma. Cho et al reported that the arc plasma can expand 4m radius from arc position [6][7].

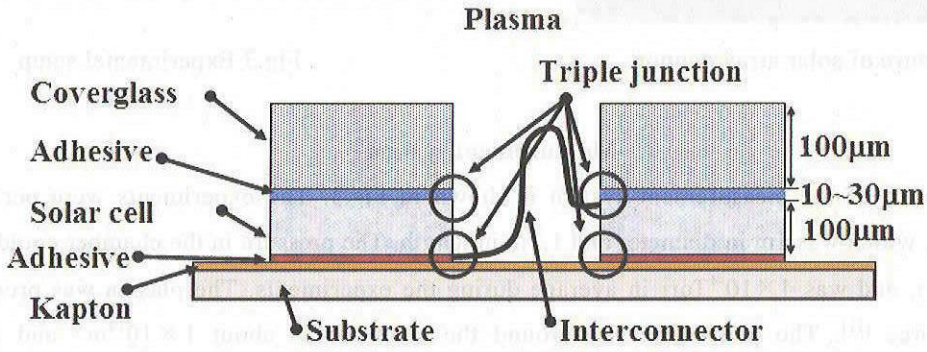

Fig.1 The cross sectional view of solar array

Cho et al [8][9] have developed high voltage solar array for 400V-bus LEO satellite. From their research, the best mitigation technique is to cover solar array from ambient plasma by thin film. When a tiny piece of debris impacts the film-covered solar array, however, there is a possibility that the film suffers a hole. The arcs may occur once the covering film is damaged. Therefore, we should not only develop mitigation technique against arc inception, but also prepare for the situation when the mitigation technique becomes ineffective. In the previous works, a solar cell was damaged by single arc, and the solar cell degradation was short-circuited between P-electrode and N-electrode of a solar cell [3]. The arc which occurred on solar cell edge could degrade the solar cell. On the other hand, arcs on the electrode, such as bus bar and interconnector, could hardly cause solar cell degradation [10]. As the next step of this study, we have performed a ground experiment to identify the threshold energy of arc which causes solar cell degradation. We discuss the result of the ground experiment in this paper.

Experiment

Solar array coupon

We made two identical solar array coupons. The picture of a solar array coupon is shown in Fig.2. The substrate is 25mm thick aluminum honeycomb covered with Carbon Fiber Reinforced Plastic (CFRP), and the top of the substrate is covered with the Kapton film®. This solar array coupon is made of 24 Silicon solar cells (70mm×35mm). All solar cells are glued on the Kapton® film. Two solar cells are connected in series by the interconnectors. We used this set as one sample, that is, each coupon has twelve samples. The solar cells

have IBF (Integrated Bypass Function), which allows the current flow from N to P electrode if the cells receive no light. The electrodes of both ends of the series connection are called bus bar. All bus bars are covered by RTV silicon in order to suppress arc inception on there.

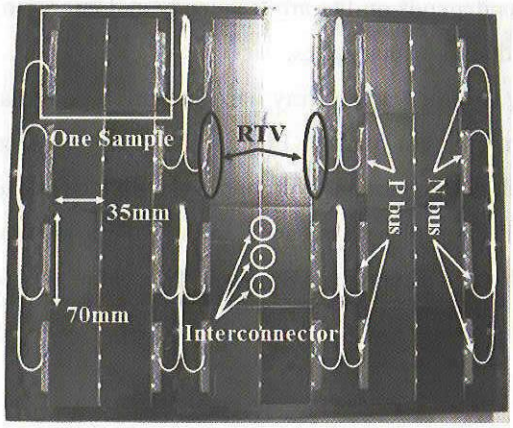

Fig.2 Picture of solar array coupon

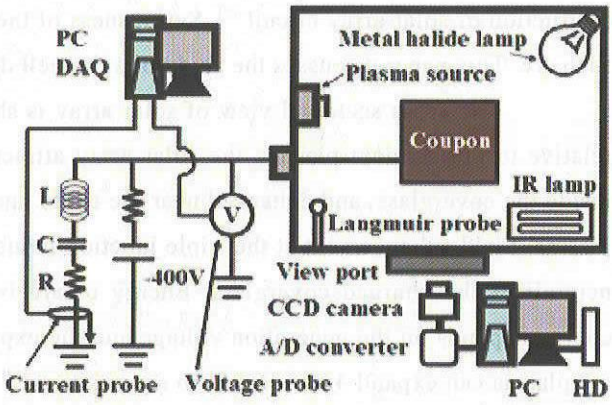

Fig.3 Experimental setup

Measurement system

The sketch of the measurement system is shown in Fig.3. The experiments were performed in a vacuum chamber, which was 1m in diameter and 1.2m in length. The pressure in the chamber could reach up to about 8×10^{-6}Torr, and was 4×10^{-4}Torr in average during the experiments. The plasma was produced by an ECR plasma source [11]. The plasma density around the coupon was about 1×10^{12}m^{-3} and the electron temperature was about 1eV with xenon gas of 0.3sccm. The coupon was kept at 40℃ by IR lamps to simulate the temperature on orbit during the experiment.

The arc location on the coupon was identified by the position identification system of arc discharge [12]. During the experiments, the video image of the coupon was recorded in a hard disk drive connected to a PC as the digital video image. After the experiments, the arc location was identified by means of analyzing the digital video image with a computer program in the PC.

All the waveforms of the array potential and the discharge current were acquired by a high speed data acquisition system. This system consists of a high speed digitizer (National Instrument, PCI5112, 20MHz), a PC and a LabVIEW program. This system can record all the waveforms even if arcs occur with a frequency of 30arcs per second.

The metal halide lamp mounted in the chamber enabled to acquire the electric performance of the coupon without opening the chamber during experiment. The energy density of this lamp was 1/500 of that of AM0. The electrical performance was acquired in each sample by measuring both the output voltage and current by shifting the value of resistance connected to the sample (VI characteristics). We obtained the output power by multiplying the output voltage by the current (VP characteristics). The example of the VI and VP characteristics are shown in Fig.4. These characteristic were measured in a sample of Fig.2.

We show the VI and VP characteristics of degraded sample in Fig.5. This characteristic was measured after the experiment on the same sample shown in Fig.4. The open voltage V_{oc} and the maximum power P_{max} decreased. This result suggests that the solar cell degradation is caused by short circuit between P-electrode and N-electrode of a solar cell. We defined the solar cell degradation as below

- Open voltage decreases 20% compared with that before experiment
- Maximum power decreases 20% compared with that before experiment

In order to distinguish the solar cell degradation, we defined reduction rate which was described by

$$Reduction\ rate = \left(1 - \frac{P_{max\_after}}{P_{max\_before}}\right) \times 100$$

where, P_{max_after} means P_{max} after experiment, P_{max_before} means P_{max} before experiment

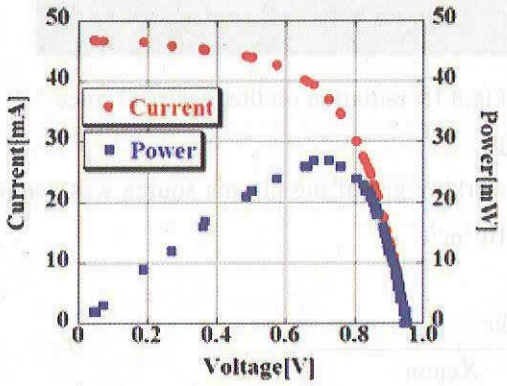

Fig.4 VI and VP characteristics of normal sample

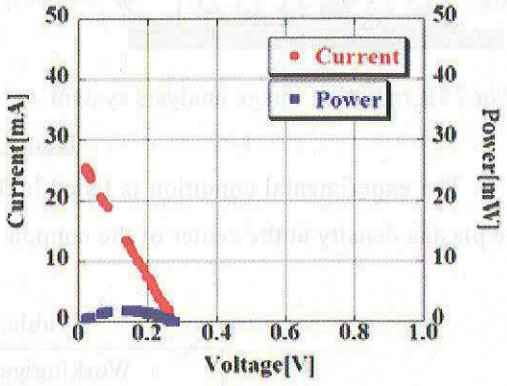

Fig.5 VI and VP characteristics of damaged sample

External circuit for experiment

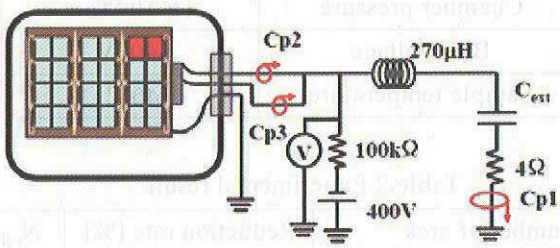

Fig.6 Experimental circuit

The external circuit used in the experiments is shown in Fig.6. This circuit is based on the experimental circuit for 400V-generation solar array ESD test in our laboratory [3].We measured the arc current by current probes (Hioki 3274, DC~10MHz or Tektronix TCPA305, DC~50MHz). We measured the coupon potential by using a high voltage probe (Tektronix P5100, DC~250MHz) or a differential probe (Tektronix P5200, DC~25MHz). The arc energy was supplied by capacitance. We changed the value of capacitance in order to change the arc energy.

IR radiation image analysis method

We developed the IR radiation image analysis method to identify the leak spot due to arcing. The conceptional diagram of this system is shown in Fig.7. When a solar cell is not irradiated with the light, it doesn't pass the inverse current because it acts as a diode. However, when the solar cell is damaged, it passes the current through the leak resistance when we apply inverse bias. The current flow through the leak resistance generates the joule heating and IR radiation. We search the IR radiation by an IR camera (Sony XC-EI50), thus we can identify the leak spot. The example image of IR radiation is shown in Fig.8.

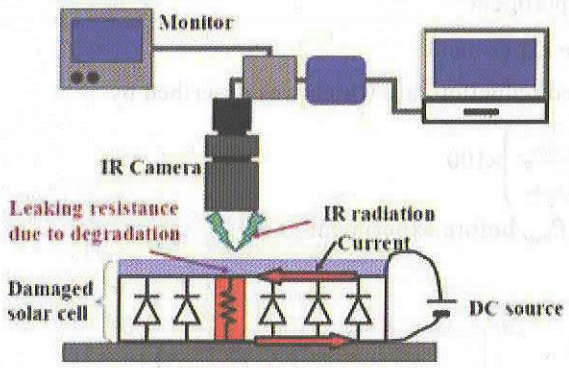

Fig.7 IR radiation image analysis system

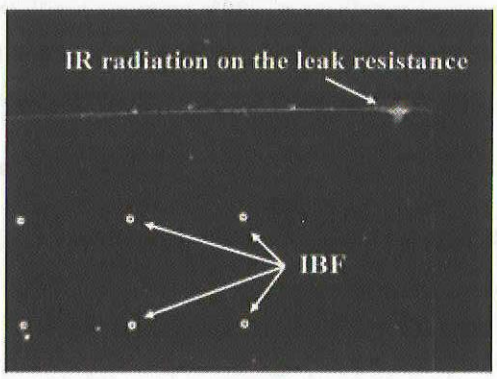

Fig.8 IR radiation on the leak resistance

Result and discussions

The experimental condition is listed in Table.1. The working gas of the plasma source was xenon, and the plasma density at the center of the coupon was about $1\times10^{12}m^{-3}$.

Table.1 Test condition

Working gas	Xenon
Mass flow late	0.3sccm
Plasma density	$1\times10^{12}m^{-3}$
Chamber pressure	4×10^{-4}Torr
Bias voltage	-400V
Sample temperature	40℃

Table.2 Experimental result

C_{ext}[F]	Number of arcs			Reduction rate [%]	N_{cell}	Number of leak spots
	N_{edge}	N_{ic}	N_{total}			
20μ	12	20	32	78	1	2
10μ	21	10	31	88	2	2
8μ	25	16	41	57	1	1
5μ	28	12	40	89	2	2
3μ	43	17	60	78	1	1
1μ	39	20	59	38	1	1
800n	61	11	72	51	1	1
613n	74	24	98	58	1	1
450n	72	28	100	20	1	2
310n	113	30	143	6.6	0	-
200n	212	43	255	10	0	0
80n	243	57	300	6.4	0	0

Table.2 shows the experimental result. Here, N_{edge} is the number of arc on the solar cell edge, N_{ic} is

the number of arcs on the interconnector and N_{total} is a sum of N_{ic} and N_{edge}. N_{cell} means the number of solar cell which suffered damage. There were two leak spots on a solar cell in C_{ext}=20μF and 450nF. In other cases, there was one leak spot on a solar cell. This fact indicates that only one arc can cause the solar cell degradation. In the case of C_{ext}=3μF, the reduction rate was 78% suggesting destruction of more than one cell. However, when we measured V_{oc} of each cell after experiment, V_{oc} of one solar cell drastically decreased, while V_{oc} of the other solar cell did not decrease. We found only one leak spot on the cell that showed the decrease of V_{oc}. Therefore, we determined that the number of damaged solar cell was one. In the case of C_{ext}=310nF, the damage of the solar cells were less than the definition. We used this sample in another experiment before performing IR radiation image analysis, then, we could not identify the number of leak spot.

One of the arc track, where we identified the current leak spot, was shown in Fig.9. The photograph was taken by tilting the microscope to 30 degree. The arc track reached the N-electrode. This fact indicated that the leak resistance was made of arc track. We identified that the arc track reached N-electrode in all the leak spots.

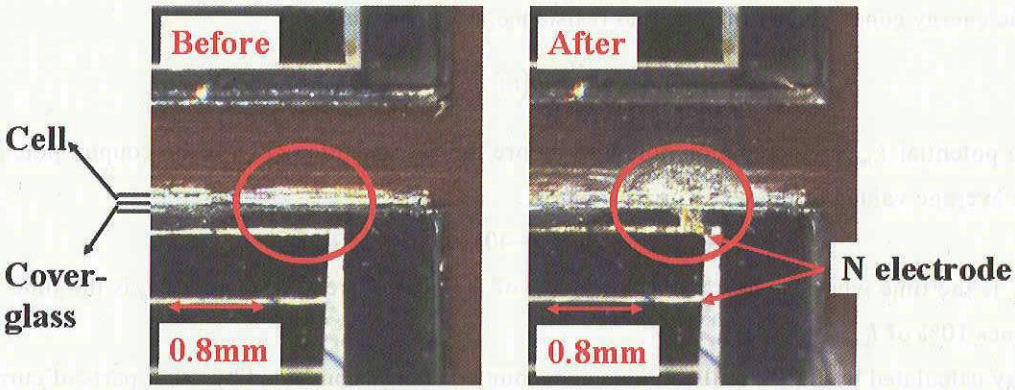

Fig.9 The microscopic picture which took arc track from a slant angle of 30 degree

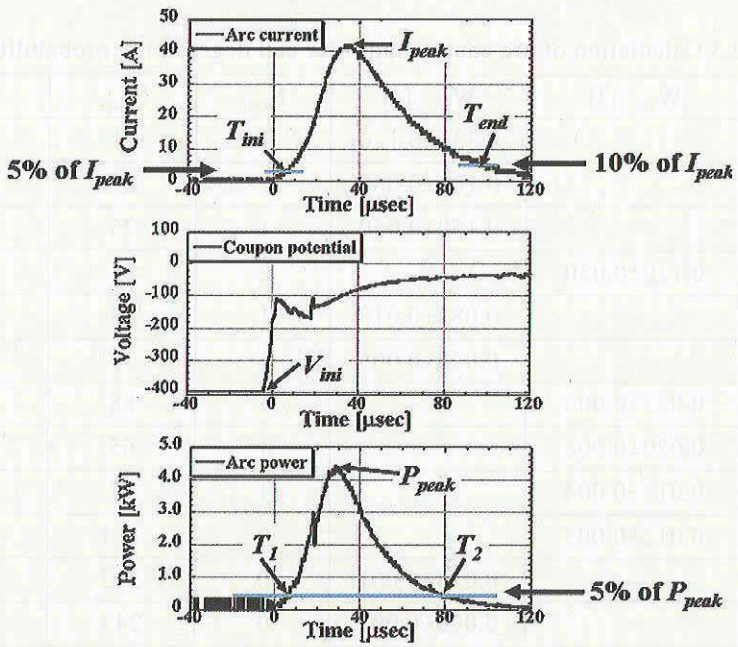

Fig.10 Arc current waveform, Potential waveform and Arc power waveform

We calculated arc energy in each capacitance. The typical current waveform and potential waveform

are shown in Fig.9. These waveforms were acquired in the case of C_{ext} = 5μF. We multiplied the arc current by the coupon potential in order to obtain the arc power waveform shown in Fig.9. We defined the time T_1, T_2 as the time when the power becomes 5% of the peak value, P_{peak}. The arc energy W_{arc_1} is written by

$$W_{arc\_1} = \int_{T_1}^{T_2} V(t) I(t) dt \qquad (1)$$

We call this calculation method as method1.

Because of malfunction of the voltage probe where high frequency response of the probe was very bad, we could not use Eq.(1) to calculate arc energy for several cases. For those cases, we used another method to calculate the arc energy. The arc energy based on this method is denoted as W_{arc_2} and defined as

$$W_{arc\_2} = W_c - W_{loss} \qquad (2)$$

where W_c is the energy released by capacitance and calculated by

$$W_c = \frac{1}{2} C_{ext} \left[V_{ini}^2 - V_{end}^2 \right] \qquad (3)$$

and W_{loss} is the energy consumed by the external resistance, 4 Ω, calculated by

$$W_{loss} = 4 \times \int_{T_{ini}}^{T_{end}} I(t)^2 \, dt \qquad (4)$$

In Eq.(3), the potential V_{ini}, is the coupon potential before the arc inception, V_{end} is the coupon potential after arc. From the average valued of the waveforms we took,

$$V_{end} = -40V$$

In Eq.(4), T_{ini} is the time when the current becomes 5% of the peak current, I_{paek}, and T_{end} is the time when the current becomes 10% of I_{peak}.

The arc energy calculated by Eq.(2) still contains unaccounted energy consumed by other parts of current path. The arc energy W_{arc_2} gives overestimate from 8mJ to 25mJ compared to W_{arc_1}.

Table.3 Calculation of arc energy and solar cell degradation probability

C_{ext}[F]	W_{arc_1}[J]	W_{arc_2}[J]	N_{cell}	N_{edge}	P_{deg}
20μ	-	0.330±0.120	1	11	0.090
10μ	-	0.180±0.060	2	21	0.095
8μ	-	0.150±0.050	1	25	0.040
5μ	0.130±0.030	-	2	28	0.071
3μ	-	0.082±0.018	1	43	0.023
1μ	-	0.045±0.005	1	39	0.025
800n	0.025±0.006	-	1	58	0.017
613n	0.020±0.006	-	1	65	0.015
450n	0.015±0.004	-	1	57	0.017
310n	0.012±0.003	-	0	113	0
200n	-	0.014±0.001	0	212	0
80n	-	0.006±0.001	0	243	0

In the case of C_{ext}=450nF, one solar cell suffered damage. However, no solar cell suffered damage for C_{ext}=310nF. We evaluated the arc energy by the method1, because the method1 was more accurate than the

method2. The arc energy was about 15mJ in C_{ext}=450nF. Then the threshold energy for Silicon solar cell degradation due to single primary arc was about 15mJ.

In Fig.11, we plot W_{arc_1}, W_{arc_2} and W_{loss} against different values of the external capacitance. Fig.11 shows that W_{arc_1} and W_{arc_2} have little difference except slight overestimate by W_{arc_2}. The energy consumed at the 4∧ resistance is smaller than W_{arc_1} and W_{arc_2} for C_{ext}<1μF and larger for C_{ext}>1μF. This means that the resistance of primary arc plasma between the arc spot and the chamber wall is larger than 4 Ω for C_{ext}<1μF and smaller than 4 Ω for C_{ext}>1μF.

We defined the time T_{ini} which was 5% of I_{peak} in Fig.10. The pulse width T_p was described by

$$T_p = T_{end} - T_{ini} \quad (5)$$

The relationship C_{ext}, I_{peak} and T_p are shown in Fig.12 and 13. Although the I_{peak} increased with C_{ext} below the C_{ext}=5μF, the I_{peak} saturated above C_{ext}=5μF. On the other hand, the T_p increased with C_{ext} in all case.

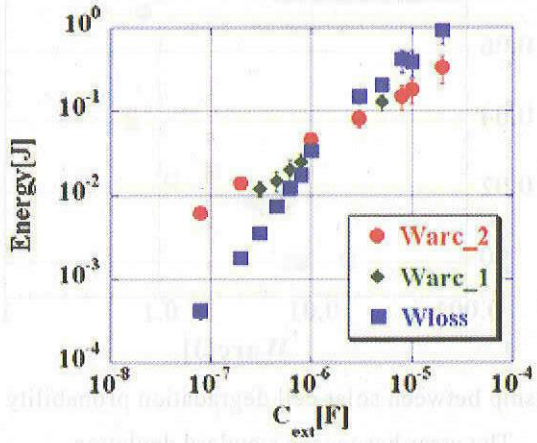

Fig.11 The changes of arc energy W_{arc} and loss energy W_{loss} depending on the capacitance

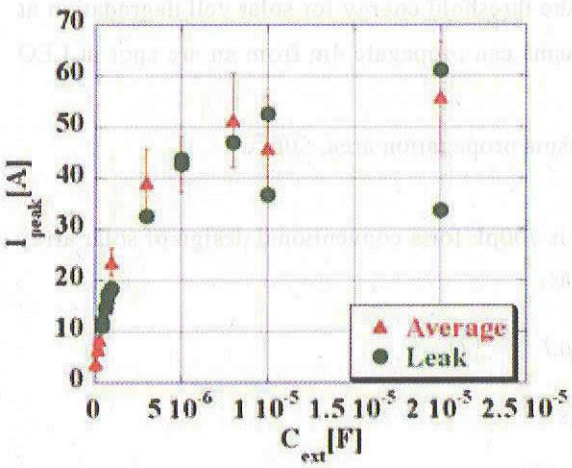

Fig. 12 The relationship between value of capacitance and I_{peak}
The error-bar means standard deviation

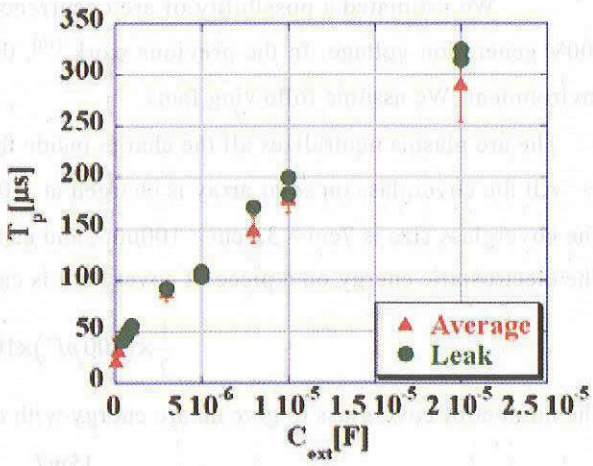

Fig.13 The relationship between value of capacitance and T_p
The error-bar means standard deviation

In Fig12 and 13, the triangle points mean the average of I_{peak} or T_p for a given capacitance. The circular points mean the arc which caused solar cell degradation. The I_{peak} increased logarithmically against capacitance, on the other hand T_p increased linearly. The arc which caused solar cell degradation had no special

value of I_{peak} and T_p.

We calculated solar cell degradation probability listed as P_{deg} in Table.3. In our previous works, arcs at electrode did not cause solar cell degradation.[10] Therefore, we considered only the arc on the cell edge. The solar cell degradation probability P_{deg} is defined as

$$P_{deg} = \frac{N_{cell}}{N_{edge}} \qquad (6)$$

The relationship between solar cell degradation probability and arc energy is shown in Fig.14. There is a strong relationship between the arc energy and the solar cell degradation probability. The higher the arc energy is, the higher the solar cell degradation probability becomes

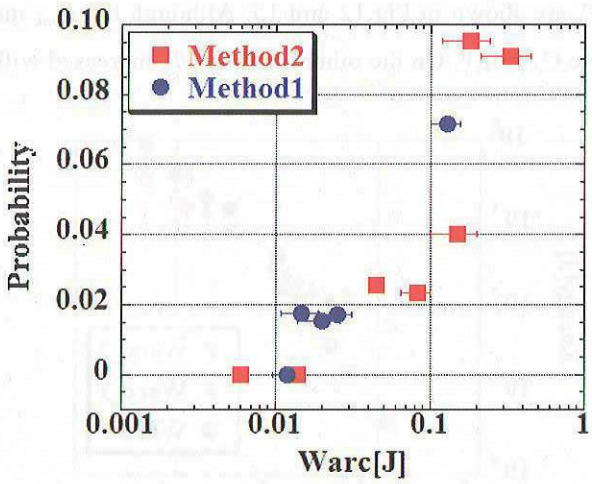

Fig.14 The relationship between solar cell degradation probability and arc energy
The error bar means standard deviation

We estimated a possibility of arc occurrence above the threshold energy for solar cell degradation at 100V generation voltage. In the previous work [10], the arc plasma can propagate 4m from an arc spot in LEO environment. We assume following facts.

- The arc plasma neutralizes all the charge inside the arc plasma propagation area, 50m^2.
- All the coverglass on solar array is charged at -100V

The coverglass size is 7cm×3.5cm×100mm, and capacitance is 700pF for a conventional design of solar array. The electrostatic energy on a piece of coverglass is calculated as

$$\frac{1}{2}\times(700pF)\times100^2 = 3.5\mu J \qquad (7)$$

The number of coverglass to give an arc energy with of 15mJ is

$$\frac{15mJ}{3.5\mu J} = 4200 \qquad (8)$$

The area of 4200 coverglass is 10m^2. Therefore, an arc that may destroy a solar cell can occur on an 100V satellite in LEO.

If the arc with energy less than the threshold occurs repeatedly on the solar cell edge, many of the high resistance leak spot may be generated and the solar cell may suffer serious degradation. We performed degradation experiment for arc energy<15mJ. We used the same sample for C_{ext}=310nF. In order to obtain high

arc frequency, we biased the -800V to sample. In order to match the electrostatic energy for C_{ext}=310nF, we changed the capacitance to 80nF. We show the test results in table.4. The W_{arc_1} was different between C_{ext}=310nF and C_{ext}=80nF, because the waveform was changed.

Table.4 The test result

Case	C_{ext}[F]	V_{bias}[V]	N_{edge}	W_{arc_1}[J]
1st	310n	-400	113	0.012±0.002
2nd	80n	-800	79	0.007±0.002
3rd	80n	-800	111	0.007±0.002
4th	80n	-800	145	0.007±0.002

We show the V_{oc} profile against primary arc number and Pmax profile against primary arc number in Fig.15, 16. The 2nd point in each plot is the data of C_{ext}=310nF experiment. Although, the decrease of V_{oc} was not observed, we searched for leak spots because the P_{max} decreased about 7% after experiment.

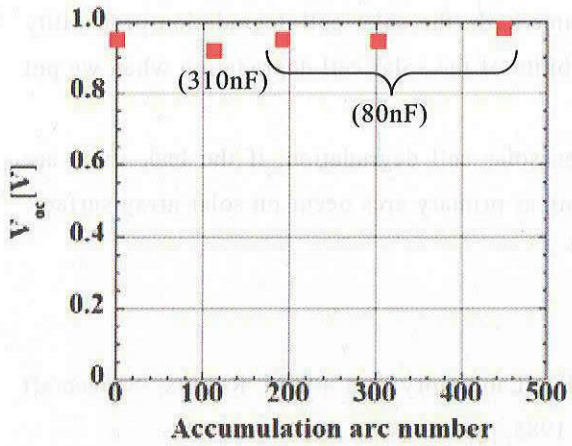

Fig.15 Profile of V_{oc} against primary arc number

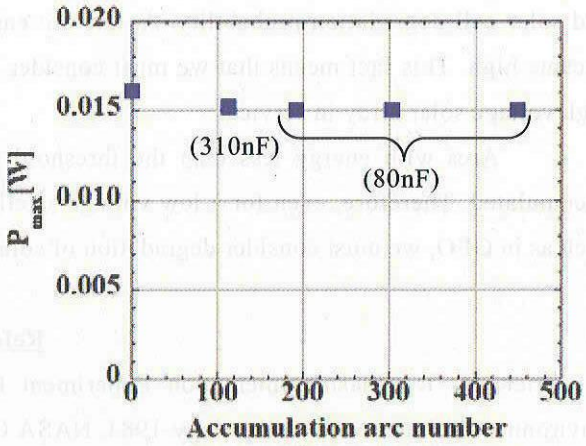

Fig.16 Profile of P_{max} against primary arc number

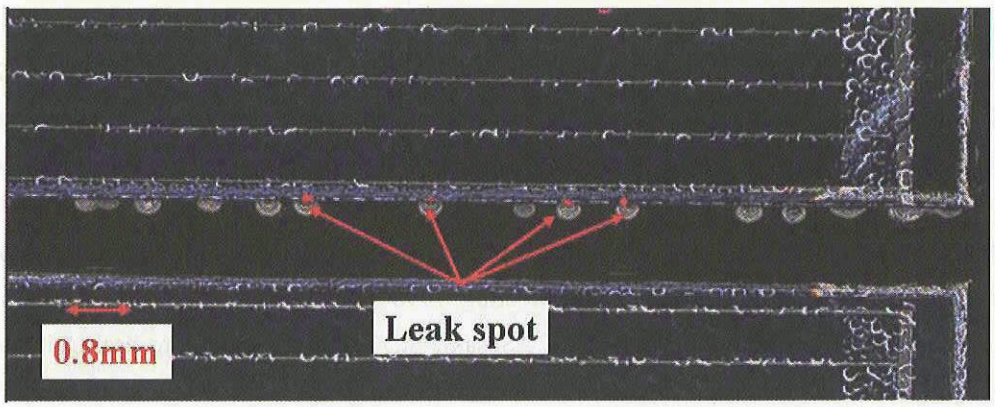

Fig .17 Compose picture of microscope and IR radiation analysis after the repeated primary arc test

We show a compose picture of microscope and IR radiation image analysis in Fig.17. We identified the decrease of P_{max} was caused by four leak spots on the arc track. We could not identify the value of

resistance on leak spot. However, this result means that the arc could generate a high resistance leak spot, even if the arc energy is below the threshold. Accumulation of high resistance leak spots may cause more serious solar cell degradation. Because the P_{max} decreased 1.8% per one leak spot, 28 of such leak spots may lower P_{max} by 50%

Conclusions

Degradation test of Si solar array was performed in a vacuum chamber simulating the LEO plasma environment. The system can measure the electrical performance of the solar array without opening the chamber. The arc energy was controlled in order to make clear the threshold arc energy that causes solar cell degradation. We developed an IR radiation image analysis system. We can identify the current leak position due to arcing using this system.

We changed the external capacitance from 80nF to 20μF. We calculated the arc energy of each capacitance. The threshold energy of degradation was 15mJ. When an arc as small as 15mJ occurred on edge of solar cell, Si solar cell may suffer damage by single arc. There was a strong relationship between the arc energy and solar cell degradation probability. As the arc energy became high, the solar cell degradation probability became high. This fact means that we must consider the possibility of the solar cell degradation when we put high voltage solar array in service.

Arcs with energy less than the threshold may cause solar cell degradation, if the leak spots are accumulated. Therefore, even for a low voltage satellite, as long as primary arcs occur on solar array surface, such as in GEO, we must consider degradation of solar cell.

References

[1] Grier, N. T.,: Plasma Interaction Experiment II (PIX II): Laboratory and Flight Results, Spacecraft Environmental Interaction Technology-1983, NASA CP-2359, 1985, pp.333-347.

[2] Hastings, D.E., Weyl, G., Kaufman, D.,: Threshold voltage for arcing on negatively biased solar arrays, 1990, Journal of Spacecraft and Rockets, September-October, pp. 539-544

[3] Okumura, T., Satoshi, H., Toyoda, K., Cho, M.,; Degradation of high voltage solar array due to arcing in LEO plasma environment, 8th SCTC Spacecraft Charging Technology Conference, Huntsville USA, 2003

[4] Toyoda, K., Matsumoto, T., Cho, M., Nozaki, Y., Takahashi, M.,; Power reduction of solar arrays due to arcing under simulated GEO environment, AIAA 2003-0628, 41st Aerospace Science Meeting, Reno USA, January, 2003

[5] Katz, I., Davis, V. A. and Snyder, D. B.,; Mechanism for spacecraft charging initiated destruction of solar arrays in GEO, AIAA 98-1002, 36th Aerospace Sci. Meeting, 1998

[6] Cho, M., Ramasamy, R., Hikita, M., Tanaka, K., Sasaki, S.,; Plasma response to arcing in ionospheric plasma environment: Laboratory experiment; 2002, J. Spacecraft and Rockets, May-June, pp.392-399

[7] Cho, M., Ramasamy, R., Hikita, M., Tanaka, K., Sasaki, S.,; Plasma response to jump of insulator surface potential in ionospheric plasma environment; 2002, J. Spacecraft and Rockets, May-June, pp.400-408

[8] Cho, M., Saionji, A., Toyoda, K., Hikita, M.,; High voltage solar array for 400V satellite bus voltage: Preliminary test results, AIAA 2003-0683, 41st Aerospace Sciences Meeting & Exhibit, Reno USA, 2003

[9] Hosoda, S., Okumura, T., Toyoda, K., Cho, M.,; High voltage solar array for 400V operation in LEO

plasma environment. 8th Spacecraft Charging Technology Conference, Huntsville USA, 2003

[10] Okumura, T., Hosoda, S., Toyoda, K., Kim, J., Cho, M.,; Degradation of high voltage solar array due to arcing in LEO plasma environment, ISTS2004-s-06, 24th ISTS International Space and Technology Symposium, Miyazaki Japan, 2004

[11] Hayashi, H., Saionji, A., Toyoda, K., Cho, M.,; Development of plasma interaction acceleration test facility for study on space material deterioration, 23rd Int. Symp. Space Tech. Sci. ISTS 2002-b-28, Matsue Japan, 2002

[12]Toyoda, K., Cho, M., Hikita, M.,; Development of automatic data recording and analysis system for laboratory experiments on high voltage solar array in space environment, Proceedings of ACED & K-J Symp. On ED and HVE, Seoul Korea, 2002, pp63-66